Journal of Solid State Chemistry **148,** 189–196 (1999)
Article ID jssc.1999.8429, available online at http://www.idealibrary.com on IDEAL®

A V(IV) Hydroxyhydrogenomonophosphate with an Intersecting Tunnel Structure: $HK_4[V_{10}O_{10}(H_2O)_2(OH)_4(PO_4)_7] \cdot 9H_2O$

F. Berrah, A. Guesdon, A. Leclaire,[1] M. M. Borel, J. Provost, and B. Raveau

Laboratoire CRISMAT, UMR 6508 associée au CNRS, ISMRA et Université de Caen, 6, Boulevard du Maréchal Juin, 14050 Caen Cedex, France

Received October 5, 1998; in revised form June 6, 1999; accepted June 29, 1999

A V(IV) hydroxyhydrogenomonophosphate $HK_4[V_{10}O_{10}(H_2O)_2(OH)_4(PO_4)_7] \cdot 9H_2O$ has been obtained, using hydrothermal conditions. Its structure, closely related to that of $(CH_3)_2NH_2K_4[V_{10}O_{10}(H_2O)_2(OH)_4(PO_4)_7] \cdot 4H_2O$, differs from the latter by its $I4_1/a$ space group (instead of $P4_3$). This difference corresponds to a "disordering" of the vanadium atoms, with respect to the dimethyl ammonium phase. It is shown that this disorder, which appears in the form of "V_5O_{22}" units distributed at random, does not affect the oxygen framework. The analysis of this complex structure shows that it can be described from the stacking along c of $[V_8P_7O_{38}(OH)_4(H_2O)_2]_\infty$ layers interconnected through layers of isolated VO_6 octahedra. In this structure, built up of VO_6, VO_5OH, and $VO_4(OH)(H_2O)$ octahedra, of VO_4OH pyramids, and of PO_4 tetrahedra, large "toffee" tunnels and smaller ones with a tulip-shape section are running along a (or b). The first ones are stuffed with H_2O molecules forming aquo tubes, where protons are likely "delocalized," whereas the second ones are occupied by K^+ cations. © 1999 Academic Press

INTRODUCTION

Anhydra vanadium phosphates in which vanadium adopts various oxidation states are currently observed (see, for example, Refs. (1–10)). In these materials, vanadium, due to its possible valence fluctuation, is susceptible to play the role of an active site for catalysis as shown for $(VO)_2P_2O_7$ (10). Besides these redox properties, the anhydra vanadium phosphates often show a tendency to form tunnels, due to the great variety of vanadium coordinations, i.e., octahedral, pyramidal, tetrahedral. Nevertheless, the so synthesized frameworks are not sufficiently open to consider these phosphates as microporous materials that would behave as zeolites (11).

The synthesis of microporous frameworks requires actually hydrothermal conditions as shown, for example, with the discovery of numerous molybdenum phosphates (12) and with the synthesis of $Na_{0.5}VOPO_4 \cdot H_2O$ (13). With the latter method, an ionic organic template is generally used in order to increase the size of the tunnels or of the cavities in the structure. In this way, Soghomonian *et al.* (14) synthesized the first vanadium phosphate containing organic template, $[(CH_3)_2NH_2]K_4[V_{10}O_{10}(H_2O)_2(OH)_4(PO_4)_7] \cdot 4H_2O$. At this point of the investigation, it is interesting to determine whether the presence of the dimethyl amine is absolutely necessary for the stabilization of such a microporous material or if this framework can be only stabilized by water, introducing oxonium ions to keep the electroneutrality. We report herein a V(IV) hydroxymonophosphate $HK_4[V_{10}O_{10}(H_2O)_2(OH)_4(PO_4)_7] \cdot 9H_2O$, hydrothermally synthesized, which exhibits a framework similar to that of $[(CH_3)_2NH_2]K_4[V_{10}O_{10}(H_2O)_2(OH)_4(PO_4)_7] \cdot 4H_2O$, although it is characterized by a different space group.

SYNTHESIS

Blue crystals of the hydroxymonophosphate $HK_4[V_{10}O_{10}(H_2O)_2(OH)_4(PO_4)_7] \cdot 9H_2O$ were grown by hydrothermal synthesis using a two-step procedure. First, a mixture of K_2CO_3, $(NH_4)_2HPO_4$, and WO_3 with the molar ratio 1:2:3 was heated in air up to 673 K. Second, the resulting product was added with powder of V_2O_5, V, and W both also in powder with the molar ratio 2.4:1.2:1. After thorough grinding, the mixture was introduced in a teflon container, with 3 cm^3 of water, heated in a steel autoclave at 220°C, under autogenous pressure, for one day, and slowly cooled down to room temperature ($2.5°.h^{-1}$). The product was filtered, washed with water, and dried in air at room temperature. The resulting green powder contains a small amount of well-formed blue square plate crystals of the title compound. The X-ray diffraction spectrum of the green powder is mainly made of the WO_3 diffraction lines.

Note that the presence of tungsten (either in the form of W or WO_3) is absolutely necessary to obtain crystals of the title compound, although no tungsten could be detected from the EDS analysis of the crystals, in agreement with the structure refinements. All attempts to synthesize

---

[1] To whom correspondence should be addressed.

0022-4596/99 $30.00

a monophasic sample were unsuccessfull; the resulting brownish powder gives an unknown diffraction pattern.

STRUCTURE DETERMINATION

A crystal of $HK_4[V_{10}O_{10}(H_2O)_2(OH)_4(PO_4)_7] \cdot 9H_2O$ with dimensions $0.128 \times 0.102 \times 0.077$ mm^3 was selected for the structure determination. The intensities recorded showed a Laue symmetry $4/m$. The cell parameters, initially measured on Weissenberg films and later refined by diffractometric technique at 293 K with a least-squares refinement based on 25 reflections, are listed in Table 1. The systematic absences $h + k + l = 2n + 1$ for hkl, $h(k) = 2n + 1$ for $hk0$ and $l \neq 4n$ for $00l$ lead to the $I4_1/a$ space group. The data were collected on a CAD-4 Enraf–Nonius diffractometer with the parameters reported in Table 1. The reflections were corrected for Lorentz and polarization effects, for absorption (Gaussian method), and for secondary extinction. The structure was solved with the heavy atom method and refined with a full matrix least-square method. The refinement of the atomic coordinates and of the anisotropic thermal factors of all atoms led to $R = 0.037$ and $R_w = 0.036$ and to the atomic parameters reported in Table 2. All the calculations were performed on a SPARC station with the Xtal3.2 chain programs (15). The refinement of the occupancy factors and the Fourier series lead to 8 vanadium atoms distributed at random over the 16 equivalent positions for each V(1), V(31), and V(32) site. Only half of these sites can be occupied, due to too short V(1)–V(1′) and V(31)–V(32) distances (about 0.7 Å).

TABLE 1
Summary of Crystal Data, Intensity Measurements, and Structure Refinement Parameters for $HK_4[V_{10}O_{10}(H_2O)_2(OH)_4(PO_4)_7] \cdot 9H_2O$

1. Crystal data	
Space group	$I4_1/a$
Cell dimensions	$a = b = 12.136(1)$ Å $c = 30.581(2)$ Å
Volume (Å)^3	4504.1(8)
z	4
ρ_{calc}(gcm^{-3})	2.36
2. Intensity measurements	
λ(Mo$K\alpha$)	0.71073
Scan mode	ω–θ
Scan width (°)	$1.0 + 0.35 \tan \theta$
Slit aperture (mm)	$1.0 + \tan \theta$
Max θ(°)	45
Standard reflections	3 measured every 3600 s
Measured reflections	9949
Reflections with $I > 3\sigma$	2300
3. Structure solution and refinement	
Refinement	on F
Parameters refined	209
Agreement factors	$R = 0.037$ $R_w = 0.036$
Weighting scheme	$w = 1/\sigma^2$
Δ/σ max	< 0.005
Δ/ρ min max	-0.76 0.73

TABLE 2
Positional Parameters and Their Estimated Standard Deviations in $HK_4[V_{10}O_{10}(H_2O)_2(OH)_4(PO_4)_7] \cdot 9H_2O$

Atom	x	y	z	B (Å^2)	Occupation
V(1)	0.2501(2)	0.2296(1)	0.75694(5)	0.62(3)	0.5
V(2)	0.26342(6)	0.23959(6)	0.42996(2)	0.94(2)	1.0
V(31)	0.1593(1)	0.1405(1)	0.86751(5)	0.84(2)	0.5
V(32)	0.1886(1)	0.1363(1)	0.84760(5)	0.84(2)	0.5
P(1)	0	1/4	1/8	1.30(5)	1.0
P(2)	0	1/4	0.79170(5)	0.62(3)	1.0
P(3)	0.24644(9)	0.60716(9)	0.33612(3)	0.76(2)	1.0
K(1)	0.1639(5)	0.221(1)	0.5586(4)	3.2(2)	0.5
K(2)	0.2024(5)	0.216(1)	0.5540(4)	3.2(2)	0.5
O(1)	0.0967(2)	0.2867(2)	0.76410(9)	0.91(6)	1.0
O(2)	0.1980(2)	0.1403(2)	0.70810(9)	1.10(6)	1.0
O(3)	0.2490(2)	0.3617(2)	0.7021(1)	1.27(7)	1.0
O(4)	0.2928(3)	0.2611(3)	0.4797(1)	2.29(8)	1.0
O(5)	0.2315(2)	0.0857(2)	0.41938(9)	1.18(7)	1.0
O(6)	0.0982(2)	0.2831(2)	0.42786(9)	0.85(6)	1.0
HO(7)	0.2639(2)	0.3782(2)	0.3987(1)	1.49(7)	1.0
O(8)	0.4069(2)	0.2032(2)	0.4034(1)	1.74(8)	1.0
O(9)	0.0906(3)	0.1571(3)	0.9116(1)	2.61(8)	1.0
O(10)	0.2077(2)	0.2945(2)	0.86114(9)	1.13(6)	1.0
O(11)	0.3078(2)	0.0987(2)	0.88683(9)	1.21(6)	1.0
H_2O(12)	0	1/4	5/8	6.9(3)	1.0
H_2O(13)	0.2382(9)	0.0821(7)	0.2585(4)	6.0(3)	0.5
H_2O(14)	0.075(1)	0.251(1)	0.2529(4)	15.0(8)	0.5
H_2O(15)	0.193(1)	0.126(1)	0.2995(4)	8.5(5)	0.5
H_2O(16)	0.236(1)	0.199(1)	0.2157(5)	12.2(6)	0.5

Note. Anisotropically refined atoms are given in the form of the isotropic equivalent displacement parameter defined as $B = 4/3 \sum_i \sum_j a_i a_j \beta_{ij}$.

The three following hypothesis may be considered to explain this statistical distribution:

(i) V(1) and V(3) are not repeated by the cell translations through the actual crystal, so that two possible oxygen–vanadium sequences can be considered:

$$\mathrm{O(9){=}V(31){-}O(3'){=}V(1){-}O(3){=}V(32){-}O(9)}$$

and

$$\mathrm{O(9){-}V(32){=}O(3'){-}V(1'){=}O(3){-}V(31){=}O(9).}$$

These two independent sequences could then be distributed at random in the whole framework.

(ii) The structure is in fact noncentrosymmetric. In that case, some extra reflections should be detected, which would allow the $I4_1/a$ space group to be discarded.

(iii) Existence of a superstructure so that extra reflections should also appear.

Weissenberg films, with long time exposure, were carefully recorded. They did not allow additional spots to be detected. Thus, the first hypothesis can be retained and will be discussed further. The refinement of the occupancy factors of the potassium atoms and of the water molecules is consistent with half occupancy except for $H_2O(12)$ which is fully occupied. This kind of occupancy seems to be related to the nature of the O(9) atoms which can be a vanadyl oxygen or a water molecule as explained below.

THERMOGRAVIMETRIC ANALYSIS

As no monophasic sample was obtained, the cleanest blue crystals of the present phase were picked out with tweezers using a binocular microscope. A first analysis performed in argon between 25 and 600°C shows a two-step loss of water. The first step between 100 and 200°C corresponds to the water molecules lying in the tunnels and the second one to the other water molecules (total $\Delta_{\mathrm{obs}} = 11\%$, $\Delta_{\mathrm{cal}} = 13\%$).

A second analysis performed in oxygen up to 700°C shows an increase of weight between 500 and 700°C corresponding to the oxidation of V^{4+} in V^{5+} ($\Delta_{\mathrm{obs}} = 3\%$, $\Delta_{\mathrm{cal}} = 4\%$).

LOCALIZATION OF HYDROGEN

The water content was confirmed by the thermogravimetric analysis. The distinction between O, OH, and H_2O was deduced from bond valence calculations performed with the Brese and O'Keeffe formulation (16). As shown from Table 3, a calculated valency ranging from 3.86 to 4.12 was obtained for vanadium, leading to V(IV). The tetravalence of vanadium was also confirmed by the weight gain, measured during the thermogravimetric analysis in air due to the oxidization of V(IV) into V(V). The analysis of the bond valence calculations shows that one valence is missing on O(7) and O(9) and two valences are missing on O(12), O(13), O(14), O(15), and O(16) (Table 3). Consequently, O(7) corresponds to a hydroxyl group OH, whereas O(12) to O(16) form H_2O molecules. The valence of 0.94 found for O(9) is

TABLE 3
Electrostatic Valence Distribution in $HK_4[V_{10}O_{10}(H_2O)_2(OH)_4(PO_4)_7] \cdot 9H_2O$

	V(1)	V(2)	V(31)	V(32)	P(1)	P(2)	P(3)	K(1)	K(2)	$\sum vi^-$
O(1)	0.5593					1.3209		0.0754	0.0489	2.005
$O(1^{i})$	0.5920					1.3209		0.0754	0.0489	2.037
O(2)	0.6385						1.2617	0.0659	0.0405	2.007
$O(2^{i})$	0.5459						*1.2617*	0.0659	0.0405	1.914
O(3)	0.2343			1.2651				0.0911	0.0734	1.664
$O(3^{i})$	1.3499		0.1887					0.0911	0.0734	1.703
O(4)		1.7169						0.1182	0.2963	1.924
O(5)		0.6667					1.2347			1.901
O(6)		0.4567	0.2302	0.2436		1.1447				2.075
			0.2302	0.2436		1.1447				
O(7)		0.6649	0.2984	0.3041						1.267
$O(7^{ii})$			0.2984	0.3041						
O(8)		0.6016			1.2447					1.846
$O(8^{iii})$					3.7341					
O(9)			0.8224	0.1223						0.945
			0.8224	0.1223						
O(10)			0.3049	0.2960			1.2823	0.0608	0.0775	2.021
			0.3049	0.2960				0.0608	0.0775	
O(11)			0.3090	0.3327			1.2181	0.0887	0.0641	2.074
			0.3090	0.3327				0.1636	0.0249	
								0.2523	0.1780	
O(12)								0.0688		0.069
								0.0688		
$O(13^{vii})$									0.0242	0.024
									0.0242	
$O(15^{xii})$								0.0236	0.0695	0.093
								0.0236	0.0695	
O(16)										
$\sum vi^+$	3.920	4.107	4.119	3.867	4.979	4.931	4.927	1.137	1.142	

Note. Symmetry codes: i, $-x + 1/2$, $-y + 1/2$, $-z + 3/2$; ii, $y - 1/4$, $-x + 1/4$, $-z + 5/4$; iii, $-x + 1/2$, $-y + 1/2$, $-z + 1/2$; iv, $x - 1/2$, y, $1/2 - z$; v, $-y + 1/4$, $x - 1/4$, $z - 1/4$; vi, $y - 1/4$, $-x + 3/4$, $z - 1/4$; vii, $-x$, $1/2 - y$, z; viii, $-y + 1/4$, $x + 1/4$, $-z + 5/4$; ix, x; $y + 1/2$; $-z + 1$; x, $y + 1/4$, $-x + 3/4$, $-z + 3/4$; xi, $-x + 1/2$, $-y + 1$, $z - 1/2$; xii, $y + 1/4$, $-x + 1/4$, $z + 1/4$.

consistent with the fact that this atom belongs half time to a vanadyl bond (BVS $\cong 1.65$) and half time to a water molecule (BVS $\cong 0.24$).

These results show that one additional charge is needed to realize the charge balance. The latter can be explained by the presence of a proton H^+. The fact that no peculiar lack of valence is detected on the other oxygen atoms of the structure suggests that $H^+$is delocalized over the different H_2O molecules of the structure.

DESCRIPTION OF THE STRUCTURE

The $[V_{10}O_{10}(H_2O)_2(OH)_4(PO_4)_7]_\infty$ framework is rather similar to that obtained for the dimethyl ammonium phosphate discovered several years ago by Soghomonian *et al.* (13), showing that the presence of an organic template is not necessary for the stabilization of such a microporous material. The projection of this structure along **a** (or **b**) (Fig. 1) shows that it consists of corner sharing VO_6 octahedra, VO_5 pyramids, and PO_4 tetrahedra forming two sorts of tunnels along **a** (or **b**), large "toffee"-shaped tunnels containing water molecules, and much smaller "tulip"-shaped tunnels where the K^+ cations are located.

Although both compounds exhibit similar crystallographic cells, they differ by their space groups: $P4_3$ for the dimethyl ammonium phase, instead of $I4_1/a$ for the present hydroxonium phosphate. As a result, the present phase differs from the first one by the positions of certain vanadium atoms, labeled V(1) and V(3) (Table 2), which are split into two half-occupied sites.

The nature of the polyhedra which form this framework can be better understood by considering that the basis of the structure consists of three corner-sharing VO_6 octahedra (one V(1) and two V(3), sharing their own edges with two VO_5 pyramids (V(2)) as depicted in Fig. 2. These groups of five vanadium polyhedra "V_5O_{22}" are then linked to each other through PO_4 tetrahedra.

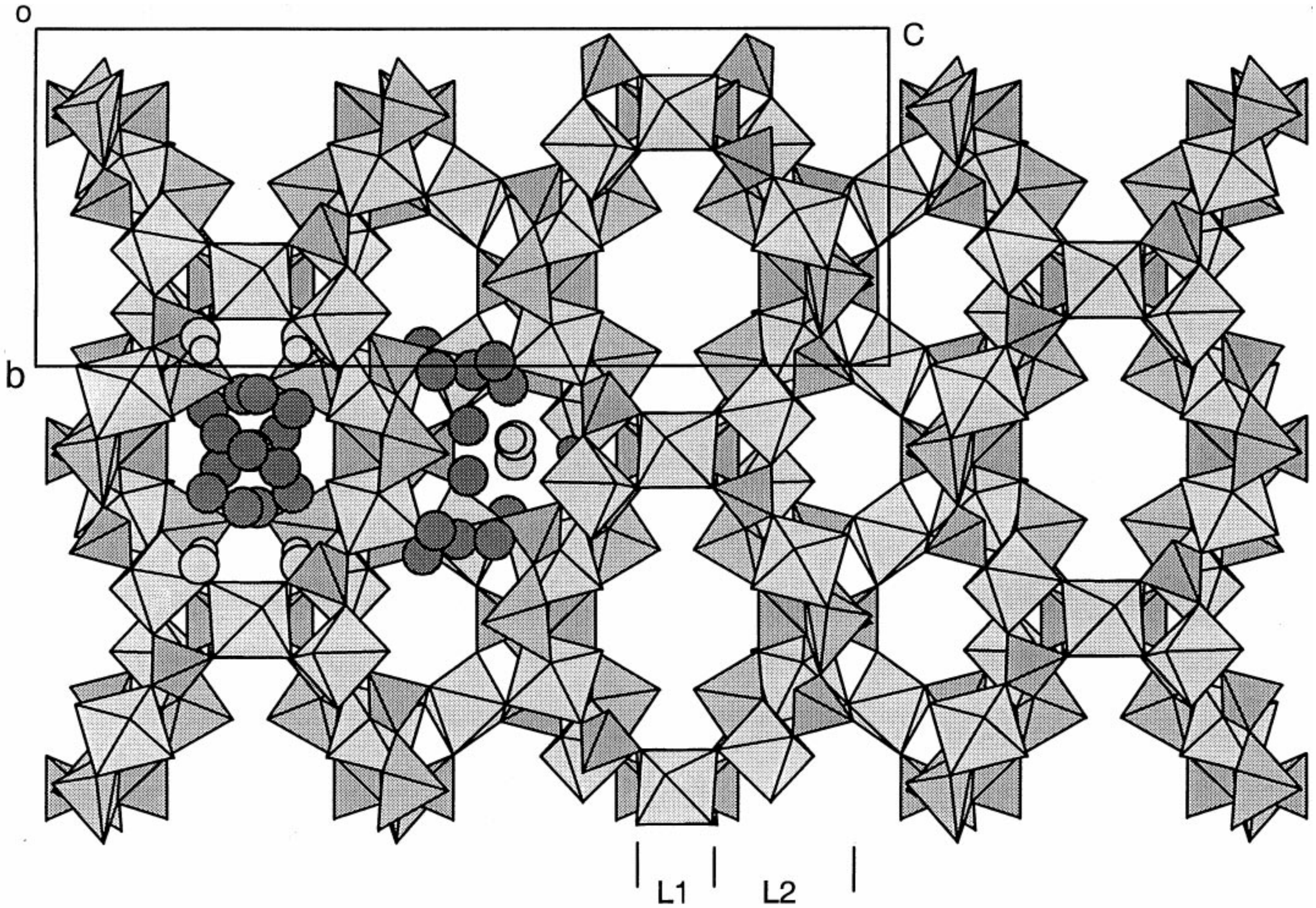

FIG. 1. Projection of the framework along **a** showing the stacking of the layers and the two sorts of tunnels. Only the potassium ions (gray circle) and the water molecules (black circle) of two tunnels are represented. L1 is the $V(1)O_6$ layer and L2 is the $[V_8P_7O_{38}(OH)_4(H_2O)_2]_\infty$ layer.

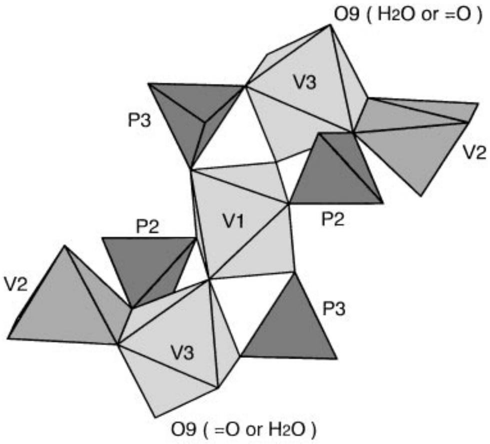

FIG. 2. The "V_5O_{22}" units sharing corners with four PO_4 tetrahedra.

The "O_6" octahedron surrounding the V(1) atom is very regular with almost similar O–O distances, ranging from 2.757 to 2.822 Å (Table 4). In this octahedron, V(1) is significantly off-centered, forming a short vanadyl bond of 1.673 Å, opposite to a long bond (2.321 Å), with the O(3) and O(3′) atoms of the two adjacent V(3) octahedra (Fig. 2). In fact the V(1) site is split into two positions which sit on both sides of the basal plane of the V(3) octahedron (O(1) O(2) O(1′) O(2′)), so that the short vanadyl V(1)=O bond may be directed toward the two surrounding V(3) octahedra (V(31) or V(32)), depending on the V(1) position.

The V(3) octahedron (V(31) or V(32)) contains one hydroxyl group (O(7)) shared with a V(2) pyramid. Its five remaining apices are either five oxygen atoms or four oxygen atoms and one H_2O molecule, depending on the occupation of the O(9) site either by an oxygen atom or by a water molecule (Fig. 2). Thus, two sites of octahedra around V(3) are observed, VO_5OH octahedra labeled V(31) and $VO_4(OH)(H_2O)$ labeled V(32) (Table 4). The V(31) and V(32) octahedra are more strongly distorted than the V(1) octahedra, with O–O distances ranging from 2.484 to 2.985 Å (Fig. 2). Note that when the O(9) site is occupied by an oxygen atom, a short vanadyl V(31)=O bond is formed (1.599 Å), whereas a long V(32)–OH_2 bond (2.305 Å) is observed (Table 4). Thus, according to the distribution of vanadium in the V(1) and V(3) sites and of oxygen and H_2O in the O(9) site, two sequences are observed in this framework: O=V(31)–O=V(1)–O=V(32)–OH_2 and H_2O–V(32)=O–V(1)=O–V(31)=O. It is remarkable that such a distribution of the V–O bonds does not disturb the rest of the framework, so that these two sequences can be distributed at random in the same framework. This "disorder" in the distribution of the trioctahedral units is fundamentally different from the perfect order observed for the dimethyl ammonium compound (14). Such a disorder is made possible by the fact that the "O_{22}" unit is centrosymmetric whereas the vanadium atoms, which are out of the center of

TABLE 4
Distances (Å) and Angles (°) in the Polyhedra in $HK_4[V_{10}O_{10}(H_2O)_2(OH)_4(PO_4)_7]\cdot 9H_2O$

V(1)	O(1)	O(1)^{i}	O(2)	O(2)^{i}	O(3)	O(3)^{i}
O(1)	**1.999(3)**	3.923(4)	2.757(4)	2.778(4)	2.801(4)	2.797(4)
O(1)^{i}	161.1(1)	**1.978(3)**	2.778(4)	2.757(4)	2.797(4)	2.801(4)
O(2)	88.5(1)	90.0(1)	**1.950(3)**	3.905(4)	2.763(4)	2.822(4)
O(2)^{i}	87.8(1)	87.5(1)	161.1(1)	**2.008(3)**	2.822(4)	2.763(4)
O(3)	80.5(1)	80.8(1)	80.1(1)	81.0(1)	**2.321(3)**	3.993(4)
O(3)^{i}	98.8(1)	99.9(1)	102.0(1)	96.9(1)	177.8(4)	**1.673(3)**
V(2)	O(4)	O(5)	O(6)	O(7)	O(8)	
O(4)	**1.584(3)**	2.912(4)	2.856(4)	2.877(4)	2.802(5)	
O(5)	111.4(2)	**1.934(3)**	2.902(4)	3.677(4)	2.608(4)	
O(6)	101.9(1)	92.7(1)	**2.074(3)**	2.484(4)	3.942(4)	
O(7)	109.3(2)	139.3(1)	76.5(1)	**1.935(3)**	2.747(4)	
O(8)	103.5(2)	83.8(1)	153.9(1)	89.4(1)	**1.972(3)**	
V(31)	O(3)^{i}	O(6)^{ii}	O(7)^{ii}	O(9)	O(10)	O(11)
O(3)^{i}	**2.401(3)**	2.751(4)	2.880(4)	3.991(4)	2.758(4)	2.845(4)
O(6)^{ii}	75.5(1)	**2.071(3)**	2.484(4)	2.825(4)	2.985(4)	3.929(4)
O(7)^{ii}	81.7(1)	75.7(1)	**1.975(3)**	2.815(5)	3.877(4)	2.792(4)
O(9)	172.2(2)	99.9(2)	103.4(2)	**1.599(4)**	2.680(5)	2.832(5)
O(10)	77.6(1)	95.3(1)	158.9(1)	96.9(2)	**1.969(3)**	2.782(4)
O(11)	80.7(1)	153.8(1)	90.3(1)	104.9(2)	90.1(1)	**1.962(3)**
V(32)	O(3)^{i}	O(6)^{ii}	O(7)^{ii}	O(9)	O(10)	O(11)
O(3)^{i}	**1.697(3)**	2.751(4)	2.880(4)	3.991(4)	2.758(4)	2.845(4)
O(6)^{ii}	94.0(1)	**2.050(3)**	2.484(4)	2.825(4)	2.985(4)	3.929(4)
O(7)^{ii}	103.3(1)	76.3(1)	**1.968(3)**	2.815(5)	3.877(4)	2.792(4)
O(9)	171.4(2)	80.6(1)	82.0(1)	**2.305(4)**	2.680(5)	2.832(5)
O(10)	97.0(1)	95.6(1)	158.6(1)	77.1(1)	**1.978(3)**	2.782(4)
O(11)	103.0(1)	161.0(1)	91.4(1)	83.4(1)	90.7(1)	**1.933(3)**
P(1)	O(8)^{iii}	O(8)^{iv}	O(8)^{v}	O(8)^{vi}		
O(8)^{iii}	**1.534(3)**	2.529(4)	2.494(4)	2.494(4)		
O(8)^{iv}	111.1(2)	**1.534(3)**	2.494(4)	2.494(4)		
O(8)^{v}	108.7(2)	108.7(2)	**1.534(3)**	2.529(4)		
O(8)^{vi}	108.7(2)	108.7(2)	111.1(2)	**1.534(3)**		
P(2)	O(1)	O(1)^{vii}	O(6)^{ii}	O(6)^{viii}		
O(1)	**1.512(3)**	2.510(4)	2.535(4)	2.488(4)		
O(1)^{vii}	112.2(1)	**1.512(3)**	2.488(4)	2.535(4)		
O(6)^{ii}	110.9(1)	107.9(1)	**1.565(3)**	2.516(4)		
O(6)^{viii}	107.9(1)	110.9(1)	107.0(1)	**1.565(3)**		
P(3)	O(2)^{ix}	O(5)^{x}	O(10)^{xi}	O(11)^{viii}		
O(2)^{ix}	**1.529(3)**	2.527(4)	2.534(4)	2.465(4)		
O(5)^{x}	111.0(1)	**1.537(3)**	2.510(4)	2.496(4)		
O(10)^{xi}	112.3(2)	110.2(2)	**1.523(3)**	2.479(4)		
O(11)^{viii}	106.8(2)	108.3(2)	108.0(2)	**1.542(3)**		

K(1)–O(3)^{ii}: 2.76(1) Å
K(1)–O(11)^{i}: 2.77(1) Å
K(1)–O(1)^{i}: 2.83(1) Å
K(1)–O(12): 2.864(9) Å
K(1)–O(2)^{viii}: 2.88(1) Å
K(1)–O(10)^{i}: 2.91(1) Å
K(1)–O(4): 2.92(1) Å
K(1)–O(11)^{v}: 3.11(1) Å
K(1)–O(15)^{xii}: 3.26(2) Å

K(2)–O(4): 2.58(1) Å
K(2)–O(10)^{i}: 2.82(1) Å
K(2)–O(3)^{ii}: 2.84(1) Å
K(2)–O(15)^{xii}: 2.86(2) Å
K(2)–O(11)^{i}: 2.89(1) Å
K(2)–O(1)^{ii}: 2.99(1) Å
K(2)–O(2)^{viii}: 3.06(1) Å
K(2)–O(9)^{i}: 3.13(1) Å
K(2)–O(11)^{v}: 3.24(1) Å
K(2)–O(13)^{xii}: 3.25(2) Å

Note. See Table 3 for symmetry codes.

their octahedra, can be displaced along the "O–V–O–V–O–V–O" bonds without any alteration of the O_{22} symmetry.

The V(2) pyramids can be formulated VO_4OH (Fig. 2). Their geometry is characteristic of V(IV) with one short vanadyl bond of 1.584 Å and four equatorial longer V–O bonds, ranging from 1.934 to 2.074 Å (Table 3). Note that each V(2) pyramid shares one edge with one V(3) octahedron and three apices with PO_4 tetrahedra (Fig. 2).

The phosphorus atoms form all PO_4 tetrahedra. P(1), which is linked to four V(2) pyramids (Fig. 3), is the most regular with four P–O bonds of 1.534 Å (Table 4). P(2), which shares two apices with two edge shared units "V(2)V(3)" (Fig. 3) and two apices with two V(1) octahedra, is significantly more distorted, with P–O bonds ranging from 1.512 to 1.565 Å (Table 4), P(3), which shares one apex with one V(2) pyramid and three apices with V octahedra (one V(1) + two V(3)), exhibits P–O bonds ranging from 1.523 to 1.542 Å (Table 4).

The complex structure of the $[V_{10}O_{10}(H_2O)_2(OH)_4(PO_4)_7]_\infty$ framework was described by Soghomanian *et al.* (14), built up of chiral double helices. In order to render an account of the 3D character of this structure we propose herein an alternative description. This framework can indeed be described by the stacking along **c** of $[V_8P_7O_{38}(OH)_4(H_2O)_2]_\infty$ layers interconnected through layers of V(1) octahedra which are not bonded each to other (Fig. 1). Each $[V_8P_7O_{38}(OH)_4(H_2O)_2]_\infty$ layer (Fig. 3) is built up from "$V_4P_3O_{21}(OH)_2OH_2$" units (Fig. 4), which share their corners and are also interconnected through P(1) tetrahedra (Fig. 3). Each unit (Fig. 4) is made by the assemblage of two V_2O_8OH or $V_2O_7(OH)(H_2O)$ subunits interconnected by PO_4 tetrahedra (1 P(2) + 2 P(3)). The V_2O_7OH (H_2O) units consist of one V(3) octahedron and one V(2) pyramid sharing one edge. Note that the H_2O molecule of this unit which corresponds to a free apex of the V(3) octahedra is directed outside of the layer. Thus, the cohesion of each layer is only ensured by oxygen atoms (neither by OH nor by H_2O). This arrangement of the polyhedra forms eight-sided windows (Fig. 3) delimited by four P(3) tetrahedra alternating with four V(3) octahedra. Along **c**, two successive $[V_8O_7O_{38}(OH)_4(H_2O)_2]$ layers, bridged by V(1) octahedra, are related to one another by a 4_1 axis, so that no tunnel runs along **c**. This description shows that the structure of this phase is characterized by a tridimensional framework whose cohesion is ensured by "single" oxygen atoms only, i.e., without H_2O and OH groups.

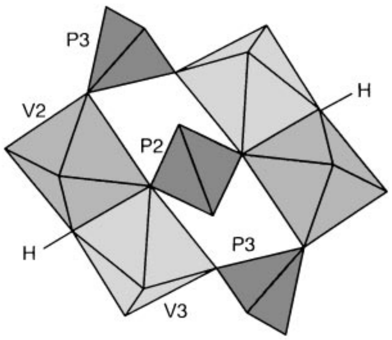

FIG. 4. The $V_4P_3O_{21}(OH)_2H_2O$ unit.

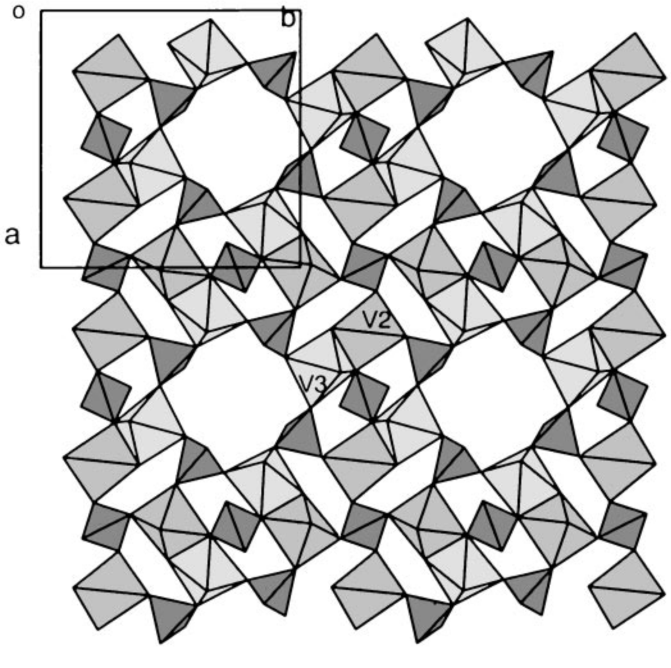

FIG. 3. The $[V_8P_7O_{38}(OH)_4(H_2O)_2]_\infty$ layer viewed along **c**.

The K^+ cations in the hydroxonium compound (Fig. 5a) are located in positions close to those of the dimethyl ammonium phase (Fig. 5b). They are distributed over two independent sites, K(1) and K(2), which are both half-occupied in the small tulip-like tunnels. In the K(1) site, potassium exhibits a monocapped distorted cubic coordination, with K(1)–O distances ranging from 2.76 to 3.26 Å. K(2) exhibits a tenfold coordination, with K(2)–O distances ranging from 2.58 to 3.25 Å (Table 3).

The H_2O molecules fill up the large toffee-like tunnels (Fig. 5a), close to the positions of H_2O in the dimethyl ammonium phase (Fig. 5b) and spreading over the space occupied by the $(CH_3)_2NH_2^+$ cations, as well as between these cationic positions. It is remarkable that the probable O–O distance between two successive H_2O molecules (ruling out the too short ones resulting from the half occupancy of the water sites) along **a** (or **b**) is rather short, ranging from 2.53 to 2.85 Å. This implies rather short hydrogen bonds and suggests that the position is not located on one particular H_2O molecule, but is mobile, running along the so-formed aquo tube.

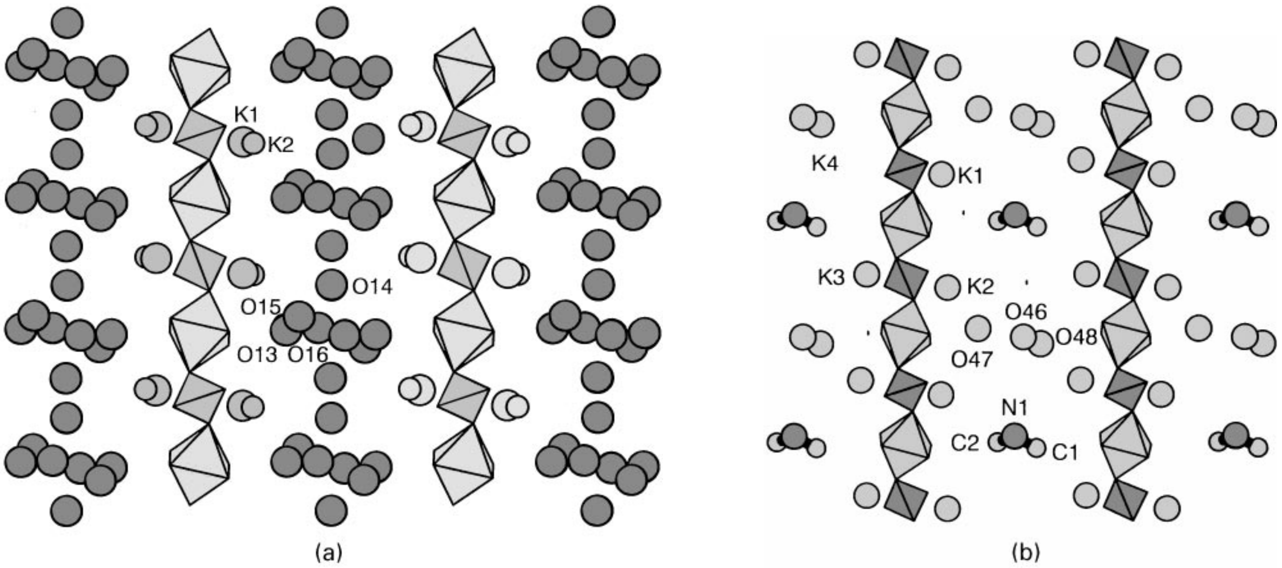

FIG. 5. The filling of the tunnels in (a) $HK_4[V_{10}O_{10}(H_2O)_2(OH)_4(PO_4)_7]\cdot 9H_2O$ and (b) $(CH_3)_2NH_2K_4[V_{10}O_{10}(H_2O)_2(OH)_4(PO_4)_7]\cdot 4H_2O$.

MAGNETIC CHARACTERIZATION

Magnetic susceptibility measurements were performed on a sample made of crystals selected with a tweezer, using a SQUID magnetometer in the 4.2–300 K temperature range, under 0.3 T.

The $\chi^{-1}(T)$ curve (Fig. 6) obeys the Curie–Weiss law, leading $C = 2.63\ \mathrm{cm^3\,K\,mol^{-1}}$ and $\theta = -3.6$ K. The obtained magnetic moment of 1.74(5) μ_B per vanadium confirms the presence of V(IV). Note that we did not find any decrease of the magnetic moment, down to 4.2 K. This behavior is different from the dimethyl ammonium phase for which the authors observe a decrease of the magnetic moment as T decreases, leading to a moment of 1.01 μ_B at 2.5 K (14).

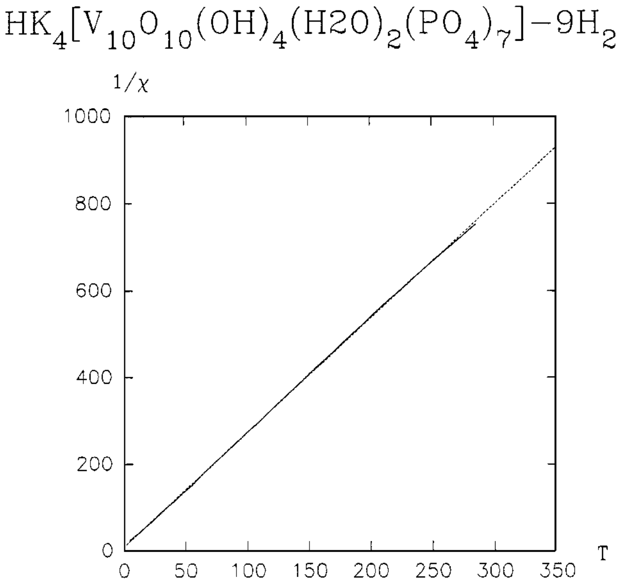

FIG. 6. Inverse molar magnetic susceptibility versus T.

CONCLUDING REMARK

A microporous V(IV) phosphate, without any organic template, showing tunnel dimensions similar to those of the dimethyl ammonium phase has been obtained. The disordering phenomena observed for the vanadium atoms show the great flexibility of this tridimentionnal framework. The existence of aquo tubes, running along **a** (or **b**) suggests the possibility of protonic conduction. Attempts to prepare large amounts of this phase will be made in order to investigate ionic conductivity.

REFERENCES

1. R. Glaum, M. Rechuis, N. Stüsser, U. Kaiser, and F. Reinauer, *J. Solid State Chem.* **126,** 15 (1996).
2. L. Benhamada, A. Grandin, M. M. Borel, A. Leclaire, and B. Raveau, *Acta Cryst. C* **47,** 424 (1991).
3. L. Benhamada, A. Grandin, M. M. Borel, A. Leclaire, and B. Raveau, *Acta Cryst. C* **47,** 2437 (1991).
4. K. H. Lii and W. C. Liu, *J. Solid State Chem.* **103,** 38 (1993).
5. W. C. Kathius, R. D. Hoffmann, J. Huang, and A. W. Sleight, *J. Solid State Chem.* **105,** 294 (1993).
6. J. W. Johnson, D. C. Johnston, H. E. King, T. R. Halbert, J. F. Brody, and D. P. Goshan, *Inorg. Chem.* **27,** 1646 (1988).
7. R. Gopal and C. Calvo, *J. Solid State Chem.* **5,** 432 (1972).
8. A. Leclaire, H. Chahboun, D. Groult, and B. Raveau, *J. Solid State Chem.* **77,** 170 (1988).

9. A. Leclaire, J. Chardon, A. Grandin, M. M. Borel, and B. Raveau, *Eur. J. Solid. State. Inorg. Chem.* **30,** 461 (1993).
10. P. T. Nguyen, R. D. Hoffman, and A. W. Sleight, *Mater. Res. Bull.* **30,** 1055 (1995).
11. M. L. Ocelli and H. E. Robson, “Zeolite Synthesis,” American Chem. Soc., Washington DC, 1989.
12. R. C. Haushalter and L. A Mundi, *Chem. Mater.* **4,** 31 (1992).
13. S. L. Wang, H. Y. Kang, C. Y. Cheng, and K. H. Lii, *Inorg. Chem.* **30,** 3496 (1991).
14. V. Soghomonian, Q. Chen, R. C. Haushalter, J. Zubieta, and C. J. O’Connor, *Science* **259,** 1596 (1993).
15. S. R. Hall, H. D. Flack, and J. M. Stewart, “Xtal3.2 Reference Manual,” Universities of Western Australia, Geneva/Maryland, 1992.
16. N. E. Brese and M. O’Keeffe, *Acta Cryst. B* **47,** 192 (1991).